

- (14) The width (peak width at half-height) of the $g_0^{\parallel} = 2.00$ peak is about 14 G for the acetato- and the formatohemins and 14 G for the individual peaks of the fluoro and bromo hyperfine patterns. This 14-G width is essentially due to unresolved ^{14}N and ^1H hyperfine structure. Chlorohemins have a peak width of about 23 G, reflecting additional unresolved chloride hyperfine structure. All of these foregoing peaks are symmetric. The peak from the azidohemin is about 40 G wide and skewed toward higher field. In work connected with ref 2c on methemoglobins with rhombic perturbations, we have previously seen such skewed $d\chi''/dH$ line shapes near $g_0 = 2.00$.
- (15) (a) J. E. Bennett, J. F. Gibson, and D. J. E. Ingram, *Proc. R. Soc. London, Ser. A*, **240**, 67–82 (1957); (b) J. E. Bennett, J. F. Gibson, D. J. E. Ingram, T. M. Haughton, G. A. Kerkrut, and K. A. Munday, *ibid.*, **262**, 395–408 (1961); (c) G. A. Helcké, D. J. E. Ingram, and E. F. Slade, *Proc. R. Soc. London, Ser. B*, **169**, 275–288 (1968).
- (16) The g_0^{\parallel} axis of the hemins upon which we are doing magnetic resonance should become slightly better oriented along the magnetic field if we can go to higher magnetic fields above the $g_0^{\parallel} = 2.00$ extremum. Of course, the EPR signal and hence the ENDOR signal very rapidly diminish in intensity above the $g_0^{\parallel} = 2.00$ extremum.
- (17) In recent measurements on OEPFeCl, which also has meso protons, we observed these intense meso proton peaks at very similar separations to those seen in proto- and deuterohemin.
- (18) (a) D. F. Koenig, *Acta Crystallogr.*, **18**, 663–673 (1965); (b) J. L. Hoard, G. H. Cohen, and M. D. Glick, *J. Am. Chem. Soc.*, **89**, 1992–1996 (1967).
- (19) (a) R. J. Kurland, R. G. Little, D. G. Davis, and C. Ho, *Biochemistry*, **10**, 2237–2246 (1971); (b) F. A. Walker and G. N. La Mar, *Ann. N.Y. Acad. Sci.*, **206**, 328–348 (1973); (c) G. N. La Mar, G. R. Eaton, R. H. Holm, and F. A. Walker, *J. Am. Chem. Soc.*, **95**, 63–75 (1973).
- (20) Quadrupole couplings are often given by the expression e^2Qq_{zz} , where eQ = nuclear quadrupole moment and eq_{zz} = z component of the electric field gradient. $e^2Qq_{zz} = 4(2I - 1)P_{zz}/3$; T. P. Das and E. L. Hahn, "Nuclear Quadrupole Resonance Spectroscopy, Academic Press, New York, N.Y., 1958, Chapter 1.
- (21) C. P. Scholes, *J. Chem. Phys.*, **52**, 4890–4895 (1970).
- (22) In ref 21 we reported for heme nitrogens that $A_{zz} = 8.18 \pm 0.34$ MHz, of which the Fermi contribution was 8.68 ± 0.16 MHz and the dipolar contribution was -0.50 ± 0.30 MHz. The Fermi interaction can be accounted for by about 2.7% of an unpaired electron in each heme nitrogen 2s orbital.
- (23) Although the intrinsic nitrogen hyperfine tensor is quite isotropic, the effective spin Hamiltonian is made highly anisotropic by the highly anisotropic g values of heme. As shown in ref 21, the magnetic hyperfine couplings increase rapidly with angle away from g_0^{\parallel} .
- (24) M. K. Mallick, J. C. Chang, and T. P. Das, *J. Chem. Phys.*, in press.
- (25) J. E. Huheey, "Inorganic Chemistry: Principles of Structure and Reactivity", Harper & Row, New York, N.Y., 1972, p 247, Table 7.4.
- (26) D. Brault and M. Rougee, *Biochemistry*, **13**, 4591–4597, 4598–4602 (1974).
- (27) THF acts through its oxygen as a weak ligand for molybdenum, as shown by: L. Ricard, P. Karagiannidis, and R. Weiss, *Inorg. Chem.*, **12**, 2179–2182 (1973).
- (28) In room temperature solutions the visible and Soret spectra of protohemin chloride change slightly in intensity and extinction upon changing in a stepwise manner from 100% CHCl_3 to 100% THF. A definite color change occurs on freezing.
- (29) See "Handbook of Chemistry and Physics", 55th ed, Chemical Rubber Publishing Co., Cleveland, Ohio, 1974, p E-69.
- (30) J. Owen and J. H. M. Thornley, *Rep. Prog. Phys.*, **29**, 675–728 (1966). See in particular p 710.
- (31) Reference 20, Chapter 7.
- (32) Reference 25, p 171, Table 4.12.
- (33) It is not surprising to find unequal intensities of the two ENDOR peaks from the same proton. An explanation for unequally intense ENDOR transitions from the same $l = 1/2$ nucleus is given by: E. R. Davies and T. F. Reddy, *Phys. Lett. A*, **31**, 398–399 (1970).
- (34) A calculation of the dipolar contribution from unpaired electron spin distributed in molecular orbitals over the entire heme is presently being done by workers of T. P. Das.
- (35) Control ENDOR experiments were done on bromohemin dissolved in 1:1 (v/v) $\text{Me}_2\text{SO}-\text{CHCl}_3$. We found that the bromide ligand was totally replaced in this solvent, and a comparison of proton ENDOR in deuterated and nondeuterated solvents showed well-defined proton ENDOR from the Me_2SO . The hyperfine interaction measured from meso protons in this solvent was $|A_{zz}| = 0.795$ MHz.
- (36) Contact shifts measured by solution NMR from methyl or $\alpha\text{-CH}_2$ groups will be motionally averaged quantities due to rapid rotation of such groups in solution. At liquid helium temperatures zero rotation may cease, and since the contact interaction varies markedly with rotation angle for such a group, different protons on the same carbon can have different contact interactions. It is conceivable that the small peaks or shoulders seen in fully deuterated solvents which lie just outside the meso proton peaks (Figures 3a,b,f) are from such immobilized protons. For a discussion of contact interaction from such protons see: A. Carrington and A. D. McLachlan, "Introduction to Magnetic Resonance", Harper & Row, New York, N.Y., 1967, Section 7.9.
- (37) An expression for the pseudocontact shift is given in eq 3, ref 19b. The pseudocontact shift depends linearly on the zero-field splitting D and inversely on T^2 , where T is the absolute temperature. There is also a dipolar geometric factor similar to eq 5 in this paper. For a D of 10 cm^{-1} at $T = 35^\circ\text{C}$ the pseudocontact shift for meso protons would be about -14 ppm; the negative sign comes from the negative sign of the geometric factor for meso protons. For proto- or deuterohemin fluorides D is about 5 cm^{-1} , and all the D values for the heme compounds used here are larger than for fluoride.³ We have calculated the change in pseudocontact interaction expected on going from deuterohemin fluoride ($D = 5.55\text{ cm}^{-1}$) to deuterohemin chloride ($D = 8.95\text{ cm}^{-1}$). This change of -5 ppm is smaller and of a different sign from the change actually seen by NMR on going from fluoro- to chlorodeuterohemin.
- (38) Reference 19b, eq 2.
- (39) Reference 36, Section 6.4.2.

Phosphorus-31 Nuclear Magnetic Resonance Chemical Shielding Tensors of L-O-Serine Phosphate and 3'-Cytidine Monophosphate

Susan J. Kohler and Melvin P. Klein*

Contribution from the Laboratory of Chemical Biodynamics, Lawrence Berkeley Laboratory, University of California, Berkeley, California 94720. Received March 22, 1977

Abstract: ^{31}P nuclear magnetic resonance chemical shielding tensors have been measured from single crystals of L-O-serine phosphate and 3'-cytidine monophosphate. The principal elements of the shielding tensors are -48 , -2 , and 51 ppm for serine phosphate and -68 , -13 , and 64 ppm for 3'-cytidine monophosphate, relative to 85% H_3PO_4 . In both cases four orientations of the shielding tensor on the molecule are possible; in both instances one orientation correlates well with the P-O bond directions. This orientation of the shielding tensor places the most downfield component of the tensor in the plane containing the two longest P-O bonds and the most upfield component of the shielding tensor in the plane containing the two shortest P-O bonds. A similar orientation was reported for the ^{31}P shielding tensor of phosphorylethanolamine and a comparison is made between the three molecules.

The recently developed high-resolution multiple pulse and cross-polarization nuclear magnetic resonance (NMR) techniques have made it possible to resolve chemical shifts in solids, and therefore to accurately determine chemical shielding tensors.^{1,2} Shielding tensors are intrinsically interesting in that

they reflect the distribution of electronic orbitals around the nucleus. Several theoretical approaches have been used with varying degrees of success to predict shielding tensors.^{3,4} On a less theoretical level, shielding tensors serve as a monitor of the chemical environment of the nucleus, and are useful in the

Table I. Values of the Principal Elements of the Chemical Shielding Tensors^a

| | Powder ^b | | | Single crystal ^c | | |
|-------------------------------------|---------------------|---------------|---------------|-----------------------------|---------------|---------------|
| | σ_{11} | σ_{22} | σ_{33} | σ_{11} | σ_{22} | σ_{33} |
| Serine phosphate | -53 | -4 | 59 | -48 | -2 | 51 |
| 3'-CMP | -63 | -9 | 71 | -68 | -13 | 64 |
| Phosphorylethanolamine ^d | -63 | -8 | 65 | -67 | -13 | 69 |

^a All values are in parts per million relative to 85% H₃PO₄, using the convention that resonances at lower field strengths have negative chemical shifts. ^b The powder values were determined by matching computer-simulated spectra with the empirical spectra; uncertainties are estimated to be approximately ± 5 ppm. ^c These are the simple numerical averages of the values from the individual symmetry-related tensors. The standard deviations were less than 4 ppm for the serine phosphate values and less than 6 ppm for the 3'-CMP values. ^d Data from ref 12.

analysis of anisotropic motion.⁵⁻¹¹ If the pertinent shielding tensor information is available, NMR spectra of anisotropic systems may be interpreted in terms of the modes of motion experienced by the molecule.

With a view toward the importance of phosphates in biological systems, especially nucleic acids and the phospholipid components of membranes, we have undertaken a study of the chemical shielding tensors of relevant organophosphates. This work reports the ³¹P chemical shielding tensors of two such compounds, L-O-serine phosphate (H₃N⁺CH(COOH)-CH₂OPO₂-OH) and 3'-cytidine monophosphate (3'-CMP), and compares them to the previously determined ³¹P shielding tensor of phosphorylethanolamine (H₃N⁺CH₂CH₂O-PO₂-OH).¹²

Experimental Techniques and Samples

Techniques. The spectrometer used for the ³¹P NMR experiments is a home-built double resonance instrument described in detail elsewhere.^{12,13} The spectrometer operates at 24.3 MHz for ³¹P detection, 60 MHz for ¹H decoupling, and is equipped with a 9.21-MHz ²H field-frequency lock.

The ³¹P Fourier transform spectra were taken using the cross-polarization nuclear enhancement technique, as described previously.^{2,12} This technique simultaneously removes the ¹H dipolar broadening and enhances the ³¹P signal by a factor of approximately two. The single contact version of this experiment was used, with a cross-polarization time of 1 ms and a ¹H decoupling field of approximately 8.6 G in the rotating reference frame. Except for the 3'-CMP single-crystal experiments, quadrature phase detection was employed.

The shielding tensors for each of the two molecules were determined from plots of resonance frequency as a function of rotation angle for three different orientations of the single-crystal samples. The methods of sample orientation and data analysis were identical with those previously described.¹³ The values of the principal elements of the shielding tensors obtained from powder spectra were determined by computer simulation and comparison with the observed spectra.

Samples. Single crystals of serine phosphate were grown at room temperature by slow evaporation from an aqueous solution originally containing 5 g of serine phosphate in 175 mL of distilled water. The crystals were harvested after 4 months. A crystal measuring 5 × 4 × 3 mm was used for the NMR experiments. The Laue precession method was used to measure the unit cell dimensions, which were $a = 7.70$, $b = 9.97$, and $c = 9.02$ Å in agreement with the literature values of $a = 7.737$, $b = 10.167$, and $c = 9.136$ Å.¹⁴

3'-CMP crystals were grown by slow evaporation from aqueous solution at room temperature. The solution originally contained 1.0 g of 3'-CMP in 50 mL of distilled water; a seed crystal was suspended in the solution to enhance crystallization. After 18 days the tabular crystals were harvested. The crystal used in the NMR experiments measured approximately 1.4 × 3 × 0.5 mm. The measured unit cell dimensions were $a = 8.75$, $b = 21.4$, and $c = 6.82$ Å, in agreement with the values of $a = 8.80$, $b = 21.7$, and $c = 6.85$ Å reported by Alver and Furberg.¹⁵

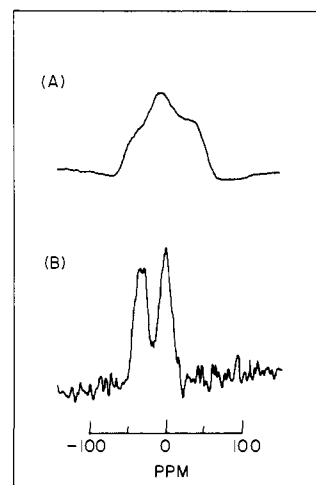


Figure 1. NMR spectra (24.3-MHz) of L-O-serine phosphate. (A) Spectrum of a powder of serine phosphate obtained from a cross-polarization experiment with ¹H decoupling; 420 passes were accumulated using a cross-polarization time of 1 ms. The scale is in parts per million relative to 85% H₃PO₄ and assumes resonances at lower field strengths have negative chemical shifts. (B) Spectrum from a cross-polarization experiment with ¹H decoupling of a single crystal of serine phosphate oriented with its *b** axis perpendicular to the magnetic field; 400 passes were accumulated. The better signal-to-noise ratio of the powder spectrum was due to the larger sample size used.

Results

Serine Phosphate. A ³¹P NMR spectrum taken of a powder of serine phosphate appears in Figure 1. The spectrum has the shape characteristically observed for a nonaxial shielding tensor, and the values measured for the three principal elements of the tensor are given in Table I. Figure 1 also shows a spectrum taken of a single crystal of serine phosphate oriented with its *b** axis perpendicular to the magnetic field. The orthorhombic symmetry (space group *P*₂₁₂₁) and presence of one serine phosphate molecule per asymmetric unit lead to a prediction that an NMR spectrum of an arbitrarily oriented crystal would have four lines; the reduction to two lines in this case is the consequence of the alignment of the crystal along a symmetry axis.

Rotation plots were generated from single-crystal spectra taken as a function of sample orientation in the magnetic field. In each case the crystal was rotated about a symmetry axis, producing spectra with two well-resolved lines and obviating the problems associated with the resolution of four resonances. Analysis of the rotation data produced four possible shielding tensors, having the same principal values and related spatially by the symmetry operations of the unit cell of the crystal. The principal values are listed in Table I, and the possible orientations of the tensors on the molecule are summarized in Table II. It is not possible on the basis of the NMR experiment alone to determine which is the proper tensor orientation; however, for reasons to be presented in the Discussion, it is judged that the orientation shown in Figure 2 (orientation 1 of Table II) is the proper choice.

3'-Cytidine Monophosphate. Spectra of powder and single crystalline samples of 3'-CMP are in general similar to those of serine phosphate. Again, the shielding tensor is nonaxial; the principal values measured from a powder spectrum are contained in Table I. As was the case for serine phosphate, 3'-CMP crystals are orthorhombic (space group *P*₂₁₂₁) and contain one molecule per asymmetric unit.¹⁵ Therefore, four symmetry-related shielding tensors were obtained from the analysis of the single-crystal data. The principal elements of the tensors are in Table I, and the possible orientations of the tensors on the phosphate molecule are given in Table II. Figure

Table II. Direction Cosines of the Principal Axes of the Tensors Relative to a Molecular Reference Frame^a

| | | Orientation 1 | | | Orientation 2 | | | Orientation 3 | | | Orientation 4 | | |
|------------------------|---------------|---------------|--------|--------|---------------|--------|--------|---------------|--------|--------|---------------|--------|--------|
| | | x | y | z | x | y | z | x | y | z | x | y | z |
| Serine phosphate | σ_{11} | -.1533 | .0706 | .9857 | -.9553 | .2720 | -.1161 | .8262 | .4535 | -.3341 | .2821 | -.7958 | -.5358 |
| | σ_{22} | .9652 | -.2032 | .1647 | .0856 | -.1217 | -.9889 | -.2053 | .7947 | .5712 | -.8456 | -.4701 | .2529 |
| | σ_{33} | .2119 | .9766 | -.0370 | -.2831 | -.9546 | .0930 | .5246 | -.4034 | .7497 | -.4532 | .3817 | -.8056 |
| 3'-CMP | σ_{11} | -.1246 | -.0368 | .9915 | -.9619 | -.1936 | -.1929 | .6793 | -.6012 | -.4209 | .4068 | .8317 | -.3780 |
| | σ_{22} | .9760 | .1752 | .1291 | .1824 | .0706 | -.9807 | -.4386 | -.7924 | .4240 | -.7191 | .5467 | .4290 |
| | σ_{33} | -.1785 | .9838 | .0141 | .2035 | -.9785 | -.0325 | -.5884 | -.1034 | -.8019 | .5634 | .0973 | .8204 |
| Phosphorylethanolamine | σ_{11} | .0038 | -.0746 | .9972 | -.9384 | .3446 | -.0235 | | | | | | |
| | σ_{22} | .9872 | .1593 | .0081 | -.1270 | -.4074 | -.9044 | | | | | | |
| | σ_{33} | -.1595 | .9844 | .0743 | -.3212 | -.8457 | .4261 | | | | | | |

^a In each case, the axis system was chosen such that the Z axis is the normal to the molecular plane containing the two shortest P-O bonds, and the X axis is their bisector. The direction cosines were calculated from the average values of the Euler angles of the equivalent tensor orientations for each molecule. These equivalent orientations were obtained by matching the symmetry-related shielding tensors with the symmetry-related molecules in the unit cell of the crystal. The standard deviations of the Euler angles were 4° or less for serine phosphate and phosphorylethanolamine and 9° or less for 3'-CMP.

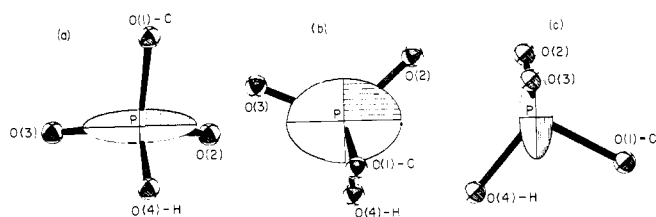


Figure 2. Chemical shielding tensor of L-O-serine phosphate. The most probable orientation of the serine phosphate shielding tensor (orientation 1 of Table II) is shown in three orthogonal projections of the phosphate region of the molecule. The shielding tensor is shown as an ellipsoid with the most downfield component of the shielding tensor represented by the shortest ellipsoid axis. The numbering of the atoms corresponds to that used in the x-ray crystallographic work.¹⁴

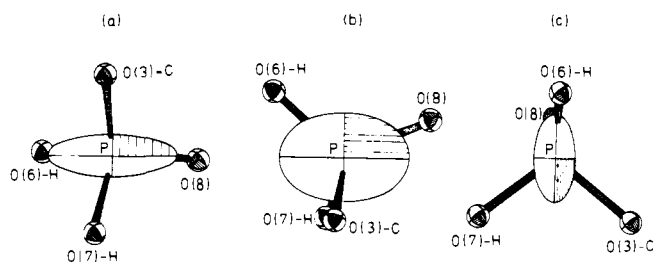


Figure 3. Chemical shielding tensor of 3'-CMP. The most probable orientation of the 3'-CMP shielding tensor (orientation 1 in Table II) is shown in three orthogonal projections of the phosphate region of the molecule. The shielding tensor is shown as an ellipsoid with the shortest axis representing the most downfield element of the shielding tensor. The numbering of the atoms corresponds to that used in the x-ray crystallographic study.¹⁵

3 diagrams the most probable orientation of the tensor (orientation 1 in Table II), as explained in the Discussion.

Discussion

The problem of matching the symmetry-related shielding tensors with the symmetry-related molecules in the unit cell of the crystal cannot be solved directly by NMR experiments,⁴ and recourse must be made to other information. In the case of the monoclinic phosphorylethanolamine (space group $P2_1/c$), there were only two possible tensor assignments, one that showed an obvious correlation with the bond directions, and one that did not.¹² The orientation which correlated with the bond directions was therefore assumed to be the proper choice. For convenience, this orientation is repeated here in Figure 4, and both possible tensor orientations are listed in Table II.

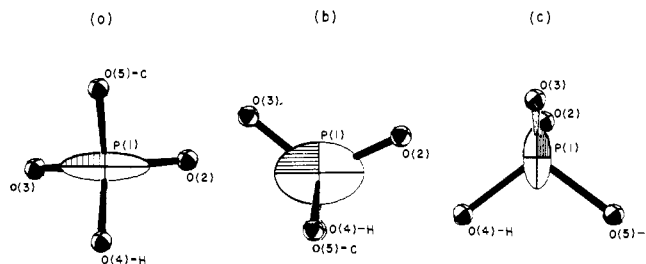


Figure 4. Chemical shielding tensor of phosphorylethanolamine.¹² The most probable orientation of the phosphorylethanolamine shielding tensor (orientation 1 of Table II) is shown in three orthogonal projections of the phosphate region of the molecule. The shielding tensor is represented as an ellipsoid with the shortest ellipsoid axis corresponding to the most downfield element of the shielding tensor. The numbering of the atoms corresponds to that used in the x-ray crystallographic study.¹⁶

Serine phosphate and phosphorylethanolamine are analogous compounds having the structure $ROPO_2OH$. One would therefore expect that these compounds should have similar orientations of their ^{31}P chemical shielding tensors. As Figures 2 and 4 and the data in Table II indicate, orientation 1 of the serine phosphate shielding tensor is similar to the phosphorylethanolamine shielding tensor orientation assumed to be correct (orientation 1 in Table II). Therefore the orientation diagrammed in Figure 2 is assumed correct in conformity with the phosphorylethanolamine results.

The question of the 3'-CMP ^{31}P chemical shielding tensor orientation is not quite as readily answered because the $RO-PO(OH)_2$ structure of 3'-CMP is not strictly analogous to the $ROPO_2OH$ structures of serine phosphate and phosphorylethanolamine. However, if one consistently chooses a molecular reference frame such that the Z axis is perpendicular to the two shortest P-O bonds and the X axis is their bisector, then it is immediately obvious that an orientation similar to orientation 1 for the phosphorylethanolamine shielding tensor may be found in all cases (orientation 1 in Table II). Therefore, in keeping with the phosphorylethanolamine and serine phosphate results, the orientation shown in Figure 3 is assumed to be the proper orientation of the ^{31}P shielding tensor in 3'-CMP.

In all three cases the most downfield component of the shielding tensor is approximately in the plane of the two longest P-O bonds (low-electron density bonds) and the most upfield component of the shielding tensor is approximately in the plane of the two shortest P-O bonds (high-electron density bonds). Recently this was also found to be the orientation for the shielding tensor of a phosphodiester, barium diethyl phosphate,¹⁷ as had been previously predicted.¹² Attempts to cal-

culate the ^{31}P chemical shielding tensors of organophosphates have not been satisfactory,¹⁸ yet the collection of empirical data from molecules of the structures ROPO_2OH , $\text{ROPO}(\text{OH})_2$, and $(\text{RO})_2\text{PO}_2$ seems to indicate that as a first-order approximation the shielding tensors of the organophosphates are aligned with the planes containing the P–O bonds. The deviations from this alignment and the variations of tensor orientation seen from molecule to molecule indicate that the ^{31}P shielding tensors are sensitive to more subtle environmental effects as well as to the P–O bond distribution, and in fact similar sensitivities have been reported for ^{13}C ^{19–21} and ^{19}F ^{7,22} chemical shielding tensors.

Acknowledgments. The authors would like to thank Helena Ruben for help in determining the crystal orientations. This research was supported in part by the U.S. Energy Research and Development Administration and in part by the National Cancer Institute (Grant No. CA 14828). S.J.K. was a Postdoctoral Fellow of the National Cancer Institute of the National Institutes of Health (Grant No. 1 F22 CA02169-01).

References and Notes

- J. S. Waugh, L. M. Huber, and U. Haeberlen, *Phys. Rev. Lett.*, **22**, 180–181 (1968).
- A. Pines, M. G. Gibby, and J. S. Waugh, *J. Chem. Phys.*, **59**, 569–590 (1973).
- U. Haeberlen, "High Resolution NMR in Solids: Selective Averaging", Academic Press, New York, N.Y., 1976, p 162.
- M. Mehring, "High Resolution NMR Spectroscopy in Solids", Springer Verlag, New York, N.Y., 1976, Chapter 5.
- S. J. Kohler and M. P. Klein, *Biochemistry*, **16**, 519–526 (1977).
- M. Mehring, R. G. Griffin, and J. S. Waugh, *J. Chem. Phys.*, **55**, 746–755 (1971).
- R. G. Griffin, J. D. Ellett, Jr., M. Mehring, J. G. Bullitt, and J. S. Waugh, *J. Chem. Phys.*, **57**, 2147–2155 (1972).
- A. Pines, M. G. Gibby, and J. S. Waugh, *Chem. Phys. Lett.*, **15**, 373–376 (1972).
- H. W. Spiess, *Chem. Phys.*, **6**, 217–225 (1974).
- H. W. Spiess, R. Grosescu, and U. Haeberlen, *Chem. Phys.*, **6**, 226–234 (1974).
- J. Seelig and H-U. Gally, *Biochemistry*, **15**, 5199–5208 (1976).
- S. J. Kohler and M. P. Klein, *Biochemistry*, **15**, 967–971 (1976).
- S. J. Kohler, J. D. Ellett, Jr., and M. P. Klein, *J. Chem. Phys.*, **64**, 4451–4458 (1976).
- M. Sundaralingam and E. F. Putkey, *Acta Crystallogr., Sect. B*, **26**, 790–800 (1970).
- E. Alver and S. Furberg, *Acta Chem. Scand.*, **13**, 910–924 (1959).
- J. Kraut, *Acta Crystallogr.*, **14**, 1146–1152 (1961).
- R. G. Griffin, manuscript in preparation.
- S. J. Kohler, unpublished results.
- R. G. Griffin, A. Pines, S. Pausak, and J. S. Waugh, *J. Chem. Phys.*, **63**, 1267–1271 (1975).
- R. G. Griffin and D. J. Ruben, *J. Chem. Phys.*, **63**, 1272–1275 (1975).
- A. Pines, J. J. Chang, and R. G. Griffin, *J. Chem. Phys.*, **61**, 1021–1030 (1974).
- R. G. Griffin, H-N. Yeung, M. D. LaPrade, and J. S. Waugh, *J. Chem. Phys.*, **59**, 777–783 (1973).

A Proton and Phosphorus Nuclear Magnetic Resonance Study of Ternary Complexes of Cyclic Adenosine 3':5'-Monophosphate, Adenosine 5'-Triphosphate, and Mn^{2+}

Sophie Fan, Andrew C. Storer, and Gordon G. Hammes*

Contribution from the Department of Chemistry, Cornell University, Ithaca, New York 14853. Received June 8, 1977

Abstract: Nuclear magnetic resonance was used to investigate the self-association of cAMP and ATP, the association of cAMP with ATP, and the interactions of the nucleotide dimers with Mn^{2+} in Tris-DCl (pH 7.6), (uncorrected meter reading) at 25 °C. The concentration dependences of the H_8 , H_2 , and H_1 proton chemical shifts of the nucleotides were used to determine association constants of 4.2 M^{-1} , 0.45 M^{-1} , and 3.0 M^{-1} for the formation of $(\text{cAMP})_2^{2-}$, $(\text{ATP})_2^{8-}$, and $\text{cAMP} \cdot \text{ATP}^{5-}$, respectively, from the monomeric species. The association constants for formation of MncAMP^+ , $\text{Mn}(\text{cAMP})_2$, and $\text{MncAMP} \cdot \text{ATP}^{3-}$ from Mn^{2+} and the nucleotides were obtained from measurements of the transverse nuclear relaxation times of the H_1 and ^{31}P nuclei of cAMP. The values obtained for the constants were 14.1 M^{-1} , 53.0 M^{-2} , and 41 700 M^{-2} , respectively. Interatomic distances between the Mn^{2+} and the H_8 , H_2 , H_1 , and ^{31}P nuclei of cAMP in the metal complexes were calculated from longitudinal nuclear relaxation times. In the $\text{Mn}(\text{cAMP})_2$ complex the metal is coordinated to the phosphate of one cAMP molecule and to the adenine ring of the other. Base stacking between the bases also occurs. A similar structure is found for the $\text{MncAMP} \cdot \text{ATP}^{3-}$ complex: the Mn^{2+} is coordinated to the triphosphate chain of the ATP and to the adenine ring of the cAMP.

Nuclear magnetic resonance has been widely used in the study of the interactions of adenine nucleotides with metals.¹ The paramagnetic ion, Mn^{2+} , binds simultaneously to the three phosphates and to the adenine ring of ATP.^{2–7} The adenine ring is separated from Mn^{2+} by a water molecule which is coordinated to the metal ion and is hydrogen bonded to N_7 of the adenine ring.^{8,9} Prior to the study reported here the interaction of cAMP with Mn^{2+} had not been studied in detail, but the interaction of cAMP with lanthanide ions has been investigated.¹⁰ (cAMP is used as an abbreviation for cyclic adenosine 3':5'-monophosphate.)

Adenine nucleotides associate in aqueous solution through base stacking,^{11–16} and the association processes involved have been investigated using several techniques including NMR^{5,17,18} and vapor pressure osmometry.¹⁹ The formation

of AMP dimers,⁵ AMP · ATP dimers,¹² and ATP dimers^{12,13} has been demonstrated. Higher aggregates are also very likely formed.^{11,13,14,19,20}

Evidence has been provided for the formation of ternary complexes consisting of adenine nucleotide dimers liganded to metal ions.^{12,16} These ternary complexes are formed by the base stacking of the two adenine rings and the metal ion binding to the phosphate(s) of one nucleotide only.^{12,16} The metal ion is then further coordinated to one or both of the adenine rings.^{12,16} For example, in the metal– $(\text{ATP})_2$ complex the metal ion binds directly (inner-sphere coordination) to the three phosphates of one of the ATP molecules and to three water molecules. The adenine rings are both outer-sphere coordinated via hydrogen bonds to two of the coordinated water molecules.¹⁶